

COHERENT MICROWAVE SYNCHROTRON RADIATION IN THE VUV RING*

S.L. Kramer[#] and B. Podobedov, BNL/NSLS, Upton, NY 11973-5000

Abstract

Microwave power, in the 3 to 75 GHz range, has been measured from beam in the VUV ring. A coherent signal was observed at frequencies below the predicted shielding cut-off of the vacuum chamber. This signal appears to be wakefields from the beam. Above the microwave instability current threshold, these fields induce modulation of the bunch current, generating intense coherent synchrotron radiation at higher frequencies.

1 INTRODUCTION

Recently several light sources [1] have observed large bursts of coherent microwave and far infrared (FIR) emission. These bursts are also observed in VUV Ring at the NSLS, as an annoying power bursts that saturate FIR detectors on the large aperture IR beam lines [2,3]. These signals appeared to be dominated by power in the ~42 GHz spectral region, that gave large amplitude bursts with a time period of 1 to 10msec when the bunch current exceeded a threshold value, I_t . Above I_t , the average power in this frequency range increased as the bunch current squared, indicating a coherent emission. The measured I_t agrees with the threshold current for the microwave instability of the bunch. A program was started to understand the source of this coherent radiation and to investigate its potential for generating high intensity FIR.

2 EXPERIMENTAL METHOD

The IR beamlines on the VUV ring use large mirrors just downstream of the dipole magnet to collect the wide angle synchrotron radiation [2]. The IR radiation is focused into an optical beam pipe, which directs the beam to one or more spectrometers. This beam pipe has a cut-off frequency of ~30 GHz, that limits the lower frequency of the FIR spectrometer. By inserting a metal blade shutter ahead of this optical beam pipe, the FIR and microwave radiation can be deflected through a glass view port into air. This allows conventional microwave components to measure the emitted radiation above the dipole vacuum chamber cut-off frequency ($f > 1.87\text{GHz}$).

The radiation in the frequency range from 3 to 75 GHz was measured using seven waveguide bands. Each band has a rectangular horn antenna to couple the radiation into a standard waveguide of at least six attenuation lengths, to filter out frequencies below the $TE_{1,0}$ cut-off frequency. Four of the waveguides have low pass filters installed in

the waveguide, to filter out frequencies above the next mode (i.e. $TE_{2,0}$ and higher suppressed). This system provided a signal selection of almost an octave frequency band for detection. This single mode signal also allowed the linear polarization of the radiation to be measured. By rotating the system 90° , the difference in polarization was measured. At frequencies below 26.5GHz quarter-wave stubs were used to couple the signal to coaxial detectors, at higher frequencies the detectors were in the waveguides. Detection of this band-selected power was done with zero bias diodes, which have high sensitivity and wide video bandwidth. This allowed observation of the power from an individual sub-nanosecond bunch. The high peak power of the bursts caused the output of these diodes to go non-linear. Consequently average power measurements were used to avoid having to compensate for this non-linearity. The spectral distribution was measured using conventional scanned RF spectrum analyzers with pre-selection filtering.

3 MICROWAVE BEAM SIGNALS

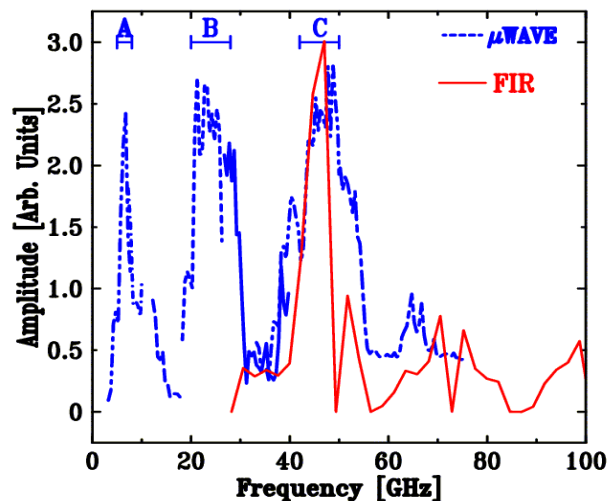


Figure 1: Frequency spectrum of the microwave and FIR signals for current above the threshold.

Fig. 1 shows the microwave spectrum measured using the RF spectrum analyzer over the 7 bands (shown by different line dashing), together with the FIR data (normalized). This spectrum was measured for currents above I_t and shows the maximum signal over a minute time period, in order to integrate over the temporal bursts. The microwave spectrum shows three peaks, labeled in Fig.1 as: A(5-8GHz), B(20-28GHz) and C(42-50GHz).

* Research supported by the US Dept. of Energy.

[#] skramer@bnl.gov

The C peak agrees with the 42GHz peak seen in the FIR data. This signal together with higher harmonics was found to result from an interference between upstream synchrotron radiation reflecting off the outer wall of the dipole vacuum chamber and the direct beam[4]. The path difference of these rays is 1cm or 30psec, creating a fringe pattern with a ~30GHz spacing and a zero (destructive interference) at ~30GHz. The FIR spectrometer could not see the first peak of this fringe pattern (see above). The microwave spectrum shows this first peak, the B peak, and the zero near 30GHz, in agreement with this model.

The coherent synchrotron radiation (CSR) has been predicted to be cut-off by electromagnetic shielding of the metallic vacuum chamber[5], at a frequency given by

$$f_c \approx \frac{c}{2} \sqrt{\frac{\rho}{h^3}}$$

for ρ the bend radius and h the vacuum chamber full height. For the VUV dipole chamber $f_c \approx 24.1\text{GHz}$, making part of the B peak below f_c . However, it was predicted[6] that there should be an enhancement of this signal above the free space CSR for $f \approx f_c$. This agrees qualitatively with the data, since the interference model predicts the B peak should be closer to 15GHz and go smoothly to zero as $f \rightarrow 0_c$, if there was no cut-off. The B peak shows a sharp decrease in signal below the peak frequency of ~20GHz.

The A peak is a major disagreement with f_c . The analysis of this A peak will be presented elsewhere[7]. In summary, the A peak appears not to be synchrotron radiation, but wakefields from vacuum chamber components, that propagate around the ring and out of this port. This is supported by: the time structure, the polarization and the low current power not in agreement with synchrotron radiation properties, unlike the B and C peaks. The shielding cut-off for synchrotron light at the A peak makes this wakefield signal possible to observe.

The properties of the B and C peaks were studied using waveguides to select one signal at a time, but only the C peak will be discussed here (B is similar). The C peak system had a nominal pass band of 33 to 50GHz, plus a 52GHz low pass filter (>40dB attenuation). The average power in this band was measured using RF power sensors. Diode sensors were used for power levels of 30pWatt to $3\mu\text{Watt}$, but they go nonlinear for peak power $>100\mu\text{Watts}$. Thermocouple sensors were used for power $>0.3\mu\text{Watts}$. These yield true average power independent of the duty cycle and peak power. Fig.2 shows the power for the C peak versus bunch current. Data from both sensors are shown to agree well in the region where they overlap. The large increase in radiation power is obvious. These data were fit with a linear current dependence (incoherent synchrotron radiation, ISR) plus an exponential rise above a current threshold to a quadratic current dependence, indicative of CSR. The threshold value for the data in Fig. 2 was $I_t \sim 102\text{ mA}$.

Previously, I_t , was shown to vary with the momentum compaction factor in agreement with the microwave instability threshold[3]. The fitted I_t variation with energy also agrees with that prediction. At 400mA (4×10^{11} electrons/bunch) the fit yields a power enhancement factor, $G = P_{tot} / P_{ISR} = 9,600$.

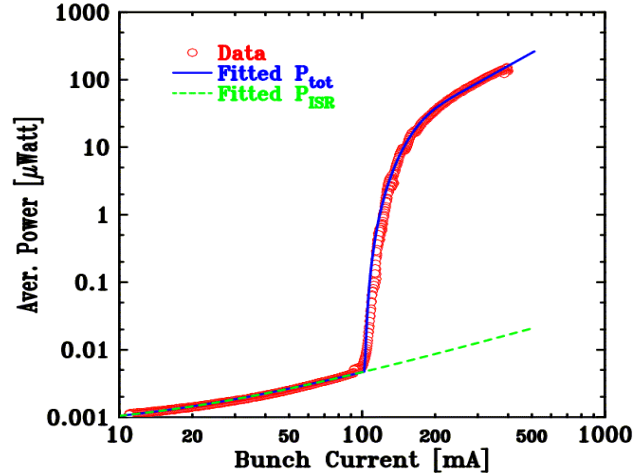


Figure 2: Average power for the C peak vs bunch current.

4 ANALYSIS OF CSR SIGNAL

The spectral dependence for CSR is given by [8]

$$P_{tot}(\omega) = N[1 + N f(\omega)] I_e(\omega) = P_{ISR}(\omega) + P_{CSR}(\omega)$$

where N = number of particles in the bunch and $I_e(\omega)$ is the power spectrum for single electrons. The bunch shape dependence enters via the form factor (spectral power density)

$$f(\omega) \equiv \left| \int_{-\infty}^{\infty} dt \exp[i\omega t] S(t) \right|^2$$

where $S(t)$ is the normalized bunch current density. For the long bunches in the VUV ring ($\sigma_t \approx 390\text{psec}$ at 400mA), $f(\omega) \ll 10^{-11}$ at both 20 and 42GHz, making CSR difficult to observe. If $S(t)$ has a modulation the form factor may become significant and CSR observable. Then G is given by $G = 1 + N f(\omega)$.

Recently a streak camera measurement of the bunch current density observed modulations on the bunch shape with a frequency of ~6.5GHz [9]. Fig. 3 shows one of these measurements, where the data was triggered on a large power burst in the A peak. The modulation is clearly observed. When the A peak power is low the bunch distribution doesn't show this modulation. Due to the high frequency noise on this data the bunch distribution was fit with a modified Gaussian distribution (to account for potential well distortion) plus a sine wave modulation (4 periods of 6.67GHz sine function with 8.5% modulation depth). This function is plotted in Fig.3 and fits the current distribution well except in the tails, which should only affect the lower frequencies.

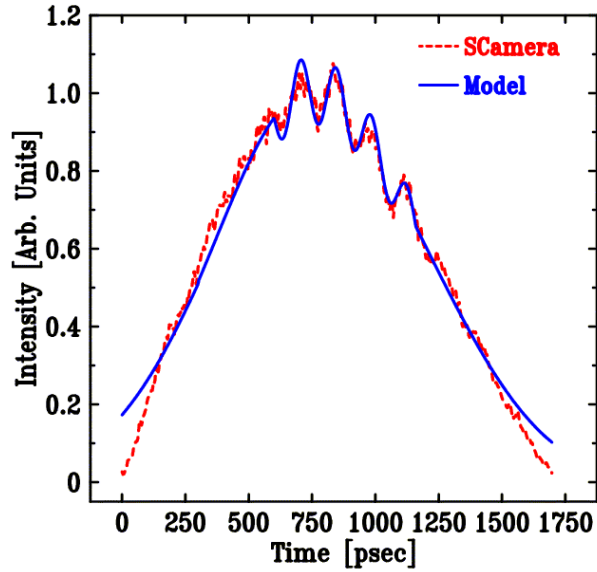


Figure 3: Measured bunch current distribution and the model (solid curve) used to estimate $f(\omega)$.

Fig. 4 shows $f(\omega)$ calculated for this model and the 512-point FFT of the streak camera data. This model predicts that at 45GHz and 400mA $f(\omega)N \approx 4 \times 10^3$, a factor of 2.4 less than the measured value.

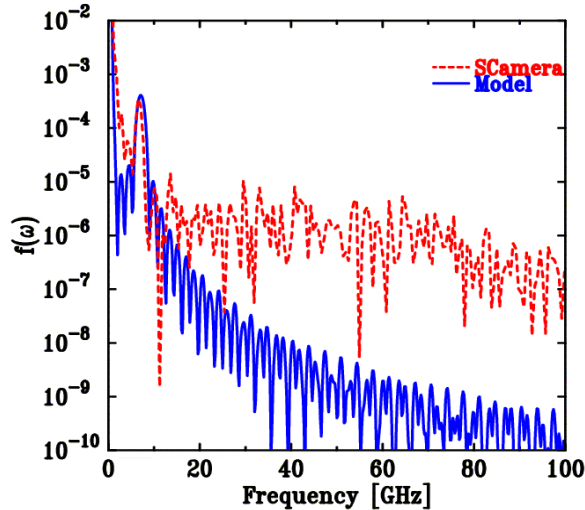


Figure 4: The form factor for the streak camera data and the bunch current model shown in Fig.3.

Since the current modulation only occurs when the power bursts occur, a duty factor must be included when comparing this estimate to the average power enhancement. The largest duty factor is the microstructure of the bunch of $\sim 300X$ (i.e. revolution period divided by bunch width), is already included in both the ISR and total power. The remaining duty factor, due to the macrostructure of the bursts, is typically of the order of 4-10X. This factor will lower the estimated G for the C peak due to this 6.6GHz modulation to 400 - 1000X. The measured value for G being greater by 9.6-24X, may indicate that other sources of C power may be present.

These might be higher frequency wakefields that could induce higher frequency micro bunching and CSR. If such fields exist, they are a small fraction of the C peak enhancement and would be difficult to observe in the presence of the A signal. This may explain why streak camera measurements have failed (so far) to observe clear micro bunching at these higher frequencies.

Study of these higher frequency wakefields might be possible by reversing the direction of this beamline. In this case the synchrotron radiation would be absorbed on the mirror back and the backward propagating wakefields in the ring could be measured. If significant wakefields are observed, then the modulation at these higher frequencies might be estimated.

The G predicted from Fig. 4 indicates the CSR should be broadband rather than peaked as in Fig. 1. The peaks however, are the result of the photon beam reflections rather than a property of the synchrotron radiation. This is supported by recent FIR data [10], that show the fringe pattern in both CSR and ISR spectra are similar.

5 CONCLUSIONS

Wakefields in peak A have been observed which, for currents above the microwave instability threshold, create a modulation of bunch current density at $\sim 6.6\text{GHz}$. The tail of this modulation appears to be the major source of CSR in the 20 and 45GHz region. If wakefields in these frequency regions are also present, their power must be considerably less than the CSR estimated for A peak modulation. The measurement of A peak wakefield was made possible due to the shielding cut-off frequency which extinguished the synchrotron radiation below 20GHz. These measurements point to a new diagnostic technique for studying the high frequency beam properties, made possible using large aperture FIR beam ports.

6 ACKNOWLEDGEMENTS

We would like to gratefully acknowledge the support of G.L. Carr in constructing and operating these FIR ports and measuring the FIR beam signals. We also thank G. P. Williams for originating the IR and CSR research at the NSLS.

7 REFERENCES

- [1] A.R. Hight-Walker, et.al., Proc.SPIE **3153**, 42(1997).
A. Andersson, et.al., Proc. SPIE **3775**, 77(1999).
M. Abo-Bakr, et.al., EPAC'00, 720(2000).
- [2] G.L. Carr, et. al., Proc. SPIE **3775**, 88 (1999).
- [3] G.L. Carr, et. al., NIM **A463**, 387 (2001).
- [4] G.L. Carr, et. al., PAC'01, (2001).
- [5] R.L. Warnock, PAC'91, 1824 (1991).
- [6] J.B. Murphy, et. al., Part. Accel. **57**, 9(1997).
- [7] S.L. Kramer, to be submitted to PRSTAB.
- [8] J.S. Nodvick and D.Saxon, Phys Rev **96**, 180(1954).
- [9] B. Podobedov, et.al., PAC'01, 1921 (2001).
- [10] G.L. Carr, private communication.